ARTICLES

Comments on the Interpretation of Dynamic Deuterium NMR Spectra from Solid Inclusion Compounds

E. Meirovitch, S. B. Rananavare, and J. H. Freed*

Baker Laboratory of Chemistry, Cornell University, Ithaca, New York 14853-1301
(Received: September 10, 1986; In Final Form: March 30, 1987)

Guest molecules trapped within the regular voids of crystalline adducts, called inclusion compounds, are likely to experience mobility. Recent solid-state ^2H NMR studies indicated these motions to be primarily discrete jumps related to the molecular symmetry, to that of the environment, or to some other geometric feature of the system investigated. In this work we offer a more consistent picture based primarily on the symmetry of the voids, but also including the molecular symmetry. We show that the ^2H NMR spectra from a whole class of guest molecules can be interpreted in terms of planar threefold jumps between unequally populated sites, such that the populations follow a simple Boltzmann law. The enthalpy difference between these sites is of the order of 1-2 kcal reflecting a rather weak but nonuniform guest-host interaction.

I. Introduction

The subject matter dealt with in this study is the dynamic structure of particular crystalline materials investigated with ^2H nuclear magnetic resonance (NMR). The recent development of experimental solid-state NMR methodologies,[1] advances in theoretical formulations of dynamic effects in NMR line shapes,[2] and progress in the chemistry of selective isotope labeling have made this technique a particularly valuable tool for studying the dynamic structure of crystalline compounds.[3]

The particular questions addressed relate to the *nature* of the mobility experienced in the solid state, as reflected in the NMR experiment and to the way it relates to molecular and environmental characteristics. To highlight those topics, which are still open to debate, and which caused us to undertake this study, we commence with a brief survey of the study of dynamics using NMR.

The basic requirements for a given motion to affect the ^2H NMR spectrum are a substantial range of spatial orientations and proper rates.[4] The former is produced by large-scale motions, the latter entails motional rates in the range of 10^3-10^{10} s^{-1}, with the region extending up to about 10^5-10^6 s^{-1} called the slow-motional regime and rates higher than 10^6 s^{-1} pertain to the motional narrowing limit. This is determined by the anisotropy of the spin Hamiltonian,[2] which for deuterium is dominated by the quadrupole interaction, with an anisotropy of the order of 2×10^5 Hz (ca. 1.3×10^6 s^{-1}). Let us focus on the liquid state, which is characterized by the Brownian tumbling of the constituent molecules, with the diffusion tensor largely determined by the molecular geometry, and the activation energy controlled by the solvent.[2] The rate of Brownian reorientation of a macromolecule with a molecular weight of roughly 50 000 au is of the order of 10^7 s^{-1} near room temperature. It is quite obvious, then, that by increasing the viscosity of the solvent by conventional techniques (such as decreasing the temperature or reasonably increasing the pressure), it will be practically impossible, as the solvent will eventually freeze, to enter the slow-motional regime with liquids. Therefore, rapid (on the ^2H NMR time scale) overall molecular reorientation will dominate fluid dynamics and will often mask segmental motions through effective isotropic motional averaging. On the other hand, by a liquid-to-solid- (or glassy) phase transition, Brownian reorientation will be quenched. Thus, if any residual motion persists it will be other than isotropic overall rotational diffusion. The nature of such motions and the physical grounds for their onset is not obvious and warrants investigation. It is our objective to gain more insight into these phenomena.

Recent dynamic NMR studies in the solid state have shown that molecules typically hop discretely, rather than diffuse continuously.[3] Numerous examples of molecules trapped within the regular vacancies of an inclusion compound lattice,[5] side chain mobility,[3,6] and bond isomerization of polymers,[3,7] etc. support

(1) (a) Mehring, M. *High Resolution NMR Spectroscopy in Solids*, 2nd ed.; Springer-Verlag: New York, 1983. (b) Haeberlen, U. *High Resolution NMR in Solids*; Academic: New York, 1976. (c) Griffin, R. G. *Methods in Enzymology*, Lowenstein, J. M., Ed.; Academic: New York, 1981; Vol. 72, Part D, Section I, p 108. (d) Skarjune, R.; Oldfield, E. *Biochemistry* **1979**, *18*, 5902.

(2) (a) Freed, J. H.; Bruno, G. V.; Polnaszek, C. F. *J. Phys. Chem.* **1971**, *75*, 3386. (b) Campbell, R. F.; Meirovitch, E.; Freed, J. H. *J. Phys. Chem.* **1979**, *83*, 525. (c) Meirovitch, E.; Freed, J. H. *Chem. Phys. Lett.* **1979**, *64*, 311. (d) Baram, A.; Luz, Z.; Alexander, S. *J. Chem. Phys.* **1973**, *58*, 4558. (e) Alexander, S.; Baram, A.; Luz, Z. *J. Chem. Phys.* **1974**, *61*, 992. (f) Alexander, S.; Baram, A.; Luz, Z. *Mol. Phys.* **1974**, *27*, 441. (g) Alexander, S.; Luz, Z.; Naor, Y.; Poupko, R. *Mol. Phys.* **1977**, *33*, 119. (h) Baram, A.; Luz, Z.; Alexander, S. *J. Chem. Phys.* **1976**, *64*, 4321. (i) Spiess, H. W. *Chem. Phys.* **1974**, *6*, 217. (j) Spiess, H. W.; Grosescu, R.; Haeberlen, U. *Chem. Phys.* **1974**, *6*, 226. (k) Pschorn, O.; Spiess, H. W. *J. Mag. Reson.* **1978**, *39*, 217.

(3) (a) Davis, J. H.; Jeffrey, K. P.; Bloom, M.; Valic, M. E.; Higgs, T. P. *Chem. Phys. Lett.* **1976**, *42*, 390. (b) Bloom, M.; Davis, J. H.; Valic, M. I. *Can. J. Phys.* **1980**, *58*, 1510. (c) Huang, T. H.; Skarjune, R. P.; Wittebort, R. J.; Griffin, R. G.; Oldfield, E. *J. Am. Chem. Soc.* **1980**, *102*, 7377. (d) Wittebort, R. J.; Schmidt, C. F.; Griffin, R. G. *Biochemistry* **1981**, *20*, 4223. (e) Jacobs, R. E.; Oldfield, E. *Prog. Nucl. Magn. Reson. Spectrosc.* **1981**, *14*, 113. (f) Wittebort, R. J.; Blume, A.; Huang, T. H.; DasGupta, S. K.; Griffin, R. G. *Biochemistry* **1982**, *21*, 3487. (g) Rice, D. M.; Wittebort, R. J.; Griffin, R. G. Meirovitch, E.; Stimson, E. R.; Meinwald, Y. C.; Freed, J. H. *J. Am. Chem. Soc.* **1981**, *103*, 7707. (h) Meirovitch, E.; Krant, T.; Vega, S. *J. Phys. Chem.* **1983**, *87*, 1390. (i) Schaefer, J.; Stejskal, E. O.; McKay, R. A.; Dixon, W. T. *J. Magn. Reson.* **1984**, *57*, 85. (j) Frey, M. H.; Opella, S. J.; Rochwell, A. L.; Gierasch, L. M. *J. Am. Chem. Soc.* **1985**, *107*, 1947. (k) Jelinsky, L. W.; Dumais, J. J.; Watnick, P. I.; Engel, A. K.; Sefcik, M. D. *Macromolecules* **1983**, *16*, 409, and references cited therein. (l) Hentschel, D.; Sillescu, H.; Spiess, H. W. *Macromolecules* **1981**, *14*, 1605. (m) Jelinsky, L. W.; Dumais, J. J.; Engle, A. K. *Macromolecules* **1983**, *16*, 403, and references cited therein. (n) Jelinsky, L. W.; Dumais, J. J.; Cholli, A. L. *Polym. Prepr. (Am. Chem. Soc., Div. Polym. Chem.)* **1984**, *25*, No. 1.

(4) Abragam, A. *Principles of Nuclear Magnetism*; Clarendon: Oxford, 1961.

(5) (a) Meirovitch, E.; Krant, T.; Vega, S. *J. Phys. Chem.* **1983**, *87*, 1390. (b) Siegel, L. A.; van den Heude, J. H. *J. Chem. Soc. A* **1967**, 817. (c) Allock, H. R.; Allen, R. W.; Bissel, E. C.; Smeltz, L. A.; Teeter, M. *J. Am. Chem. Soc.* **1976**, *98*, 5120. (d) Meirovitch, E.; Belsky, I.; Vega, S. *J. Phys. Chem.* **1984**, *88*, 1522. (e) Meirovitch, E.; Belsky, I. *J. Phys. Chem.* **1984**, *88*, 4308. (f) Meirovitch, E. *J. Phys. Chem.* **1984**, *88*, 6411. (g) Meirovitch, E.; Belsky, I. *J. Phys. Chem.* **1984**, *88*, 6407. (h) Meirovitch, E. *J. Phys. Chem.*, in press.

0022-3654/87/2091-5014$01.50/0

this statement. In some cases, such as internal methyl rotation,[8] the reorienting of a benzene ring,[6,9] and other highly symmetric structures,[10] the symmetry of the reorienting moiety appears to determine the symmetry of the motion. Thus, methyl groups reorient via discrete jumps between three orientations,[8] benzene ring residues via 180° jumps,[6] and free benzene via sixfold jumps about the hexad axis.[9] On the other hand, in many cases it is not obvious whether the exchanging sites are equally populated or whether these simple models are adequate.[3,5] For example, we found with perdeuteriated benzene trapped within the channels of a cyclyphosphazene inclusion compound that the benzene rings experience, besides the well-known rapid spinning about the hexad axis,[9] a very effective (in terms of motional averaging) large-scale motion.[5,6] Careful line-shape analysis revealed this additional motional averaging to be due to discrete planar jumps of the symmetry axis between three equally populated sites, imposed on the entrapped benzene molecule by the restrictive crystal fields set up by the host lattice. The X-ray structure of the cyclophosphazene–benzene adduct was investigated as early as 1967[5b] and further refined in 1976.[5c] In the earlier study, the resolution was insufficient to define accurately the side group parameters or to identify the location of the guest molecules in the lattice. In the later study, Fourier maps were generated for the benzene guest, indicating that electron density was located along the symmetry axis of the tunnels with the strongest residual density occupying a three-lobed area. Attempts to rationalize this residual density in terms of the known shape of the benzene molecule were unsatisfactory, indicating considerable molecular motion. Although the precise structure of host side groups pointing into the tunnel void could not be determined, these results point to a three-minimum potential energy profile prevailing at the site of the guest. This picture is compatible with the threefold jump executed by the benzene rings.[5d] No doubt, the symmetry of the environment is important in this case.

The cyclophosphazene–benzene study was extended to encompass a range of guest molecules.[5e] Also, other channel-type inclusion compounds of similar site symmetry, such as urea,[5g] thiourea,[5a] deoxycholic, and apocholic acid adducts[5h] were also investigated. In all cases, the motions detected were of the discrete jump-type, rather than diffusive. Unfortunately, in many cases only motionally narrowed spectra could be obtained and they reflect average properties only, thus containing less information than slow-motional spectra. The analysis of the experimental spectra proceeded along conventional lines, invoking simple models.

Whenever plausible on geometric grounds, exchange between two molecular orientations, which is formally identical with a 180° flip motion about a symmetrically oriented jump axis, was considered. For example, *p*- and *o*-xylene could be visualized as flipping about their molecular symmetry axes, and of the methyls in acetone to exchange through hopping about the C=O bond. In many cases, however, the fit between theory and experiment was unsatisfactory and further assumptions were required. Allowing for unequal populations is the most straightforward extension but is unjustified by the molecular symmetry.

We suggest below a more realistic and complete approach including both site and molecular symmetries. Namely, we incorporate the structure of the inclusion channels or, more specifically, the site symmetry of the host lattice, along with the geometry of the mobile molecules, to be the determinants of the dynamic behavior. Profiles of channel cross sections of the various inclusion compounds we consider below imply three minima in the potential free-energy surface; then we expect that, constrained by the host lattice, guest molecules will hop among these three minima, and this process will be augmented by any symmetry about the molecular axis. In fact, the overall symmetry group for the motional process will be seen to belong to the direct product group of the site and molecular symmetry groups.[15,16] Differences between the various adducts are assigned to variations in the relative depth of these three minima which can be rationalized in terms of nonuniform guest–host interactions.

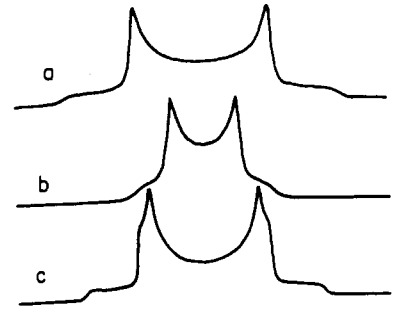

Figure 1. (a) Axial rigid-limit powder spectrum obtained with a quadrupole constant Q_0 = 165 kHz and a natural line width T_2^{*-1} = 0.21 kHz. (b) Partially averaged powder spectrum obtained by allowing the C–D bond associated with trace a to spin rapidly about a diffusion axis orthogonal to the C–D bond (i.e., $|(1/2)(3\cos\beta' - 1)| = 0.5$. (c) Asymmetric rigid-limit powder spectrum obtained with Q_0 = 165 kHz, η = 0.205, $T_2^{*-1}(x) = T_2^{*-1}(y)$ = 2.4 kHz, and $T(z)$ = 4.7 kHz (x, y, and z denote the principal axes of the quadrupole tensor).

The simplicity of this approach in providing a common interpretation is quite appealing. The method of spectral analysis is simple and straightforward, as we only need to consider (partially averaged) spectra which belong to the motional narrowing limit.

It is expected that additional experimental data, supplied by other types of solid-state NMR experiments, observing nuclei such as ^{13}C, ^{31}P, ^{1}H, ^{17}O, ^{14}N, ^{15}N, etc. and employing other techniques will both corroborate and complement this approach.

In the background section II we briefly summarize the main spectral consequences of the combined guest–host symmetry for rapid planar jumps and the effect of allowing for unequally populated sites. The presentation of our results and their discussion appears in section III and our conclusions are given in section IV.

II. Theoretical Background and Models

The main anisotropic term in the spin Hamiltonian of a deuterium nucleus in a solid is the secular part of the quadrupolar interaction.[2a,11] The NMR powder spectrum of a carbon-bonded deuterium atom with the C–D bond oriented at an angle β with respect to the external field H_0 is (assuming, for the sake of simplicity, that the quadrupolar tensor is axially symmetric) a doublet with a splitting:[2a,11]

$$\omega_L = (3e^2qQ_0/2h)(1/2)(3\cos^2\beta - 1) \qquad (1)$$

in frequency units. e^2qQ/h is the quadrupole constant Q_0 of the axial tensor Q_0 (i.e. $Q_{xx} = Q_{yy} = -1/2Q_{zz}$ and $Q_{zz} = Q_0$). For a polycrystalline morphology the spectrum will be given by properly weighted superimposed doublets, resulting in a typical pattern such as that illustrated in Figure 1a, obtained with Q_0 = 165 kHz and a natural line width T_2^{*-1} = 0.21 kHz. The spectrum is symmetric about the Larmor frequency ν_0 and the dominant features of this line shape are two strong peaks disposed symmetrically about ν_0 and separated by $\delta_0 = (3/4)Q_0$ and two extreme shoulders separated by $2\delta_0$, the former corresponding to β = 90° orientations (we shall refer to these as the "perpendicular peaks") and the latter to β = 0° orientations (to be called the "parallel peaks").

Let us also consider an asymmetric quadrupolar tensor with principal values Q_{xx}, Q_{yy}, and Q_{zz}.[1] The powder pattern is then determined by two scalar parameters, $Q_{zz} = Q_0$ and η, with η defined as $(Q_{xx} - Q_{yy})/Q_{zz}$ and $|Q_{xx}| > |Q_{yy}| > |Q_{zz}|$.[1] An example

(6) Rice, D. M.; Witebort, R. J.; Griffin, R. G.; Meirovitch, E.; Stimson, E. R.; Meinwald, Y. C.; Freed, J. H.; Scheraga, H. A. *J. Am. Chem. Soc.* **1981**, *103*, 7707.
(7) Jelinsky, L. W.; Dumais, J. J.; Engel, A. K. *Macromolecules* **1983**, *16*, 492, and references cited therein.
(8) Barnes, R. G. In *Advances in Nuclear Quadrupole Resonance*, Vol. 1, Smith, J. A. S., Ed.; Heyden: London, 1972; Chapter 26.
(9) Wemmer, D. E. Ph.D. Thesis, University of California, Berkeley, CA, 1978.
(10) Schwartz, L.; Meirovitch, E.; Ripmeester, J. A.; Freed, J. H. *J. Phys. Chem.* **1983**, *87*, 4453.
(11) See, for example, Hsi, S.; Zimmermann, H.; Luz, Z. *J. Chem. Phys.* **1973**, *69*, 4126, and references cited therein.

of such an asymmetric powder pattern is shown in Figure 1c. For this case, we may generalize eq 1 to

$$\omega_L = Q_{xx} \cos^2 \alpha \sin^2 \beta + Q_{yy} \sin^2 \alpha \sin^2 \beta + Q_{zz} \cos^2 \beta \quad (2)$$

where α and β are the Euler angles needed to describe the transformation of the principal axis system of Q into the lab frame defined by $B_0\hat{k}$, the dc magnetic field.

Since the quadrupole tensor is traceless, isotropic motion will lead to complete collapse of the quadrupole structure to give, in the motional narrowing regime, a single line centered at ν_0. When, however, there are rapid jumps between different but discrete molecular orientations or between different lattice sites, the spectral averaging will be incomplete. A new powder pattern will be observed in which the motionally averaged **Q** tensor will be reduced in magnitude. If the motional averaging is symmetric about some (molecular) axis, then an axially symmetric pattern like Figure 1a, but with reduced splitting δ will emerge. If such a symmetry is lacking in the overall averaging, then an asymmetric pattern like Figure 1c, but of narrower overall width, will emerge. In general then, the effects of rapid but partial averaging over the distinct molecular orientations due to jumps about a molecular axis and/or jumps between host sites may be written for the secular term as

$$Q_0 = \omega_L = \sum_{M,K} D^2_{OM}(\alpha,\beta,\gamma)\, \overline{D^2_{MK}(\alpha',\beta',\gamma')} Q_K \quad (3)$$

where the super bar over the Wigner-rotational matrix element D^2_{MK} implies the motional averaging over all sites i. That is

$$\overline{D^2_{MK}(\alpha',\beta',\gamma')} = \sum_{i}^{\text{all sites}} p_i D^2_{MK}(\alpha_i',\beta_i',\gamma_i')$$

where p_i is the probability of the ith orientation and the Euler angles α_i', β_i', γ_i' refer to the transformation from the PAS of **Q** in its ith orientation to the local axis system associated with the host (HAS) while the Euler angles α, β, γ represent the transformation from the HAS into the laboratory frame. Since **Q** is itself axially symmetric in its PAS, then $Q_K = 0$ except for $K = 0$, and eq 3 becomes

$$\omega_L = \frac{4\pi}{5} \sum_M Y^{2*}_M(\beta,\gamma)\, \overline{Y^2_M(\beta',\gamma')} Q_0 \quad (4)$$

A typical case will be a planar jump motion about a molecular symmetry axis; then β' is the fixed angle between this motional axis and the principal axis of $\mathbf{Q}_0$, while α_i' expresses the angle of rotation in the ith site, so $Y^2_M(\alpha',\beta') \propto P^L_{|M|}(\beta)e^{iM\alpha'}$.

$$\omega_L = \sum_i P_i(Q_0[P_2(\cos\beta)P_2(\cos\beta') - (3/4) \times$$
$$\{\sin 2\beta' \sin 2\beta \cos(\gamma_i' + \alpha) - \sin^2\beta' \sin^2\beta \cos^2(\gamma_i' + \alpha)\}] \quad (5)$$

More generally, one must consider how β_i' and γ_i' are averaged by the jumps. Here one must be guided by the molecular and host symmetries. In fact, as will be illustrated below, the overall symmetry, with regard to which the motion must be considered, will be a direct product group formed from the group of molecular symmetry operations and the host symmetry group.[15] For example, molecular C_2^M symmetry with C_3^H host site symmetry yields the $C_2^M \times C_3^H$ direct product group, which is easily found to be *isomorphous* with the simple C_6 group (and if the symmetry axes associated with the molecule and the host are parallel, then there will be an equivalence with the C_6 pure rotational group). Not all of the group symmetry operations will correspond to feasible jumps, so only the subgroup corresponding to feasible motions needs to be considered.[16] This is illustrated with the cases discussed below. In these models we shall allow for a distortion of the symmetry so that averaging over the host sites is not necessarily uniform. Nevertheless, we shall base the *selection* of jump sites upon the undistorted symmetry group.

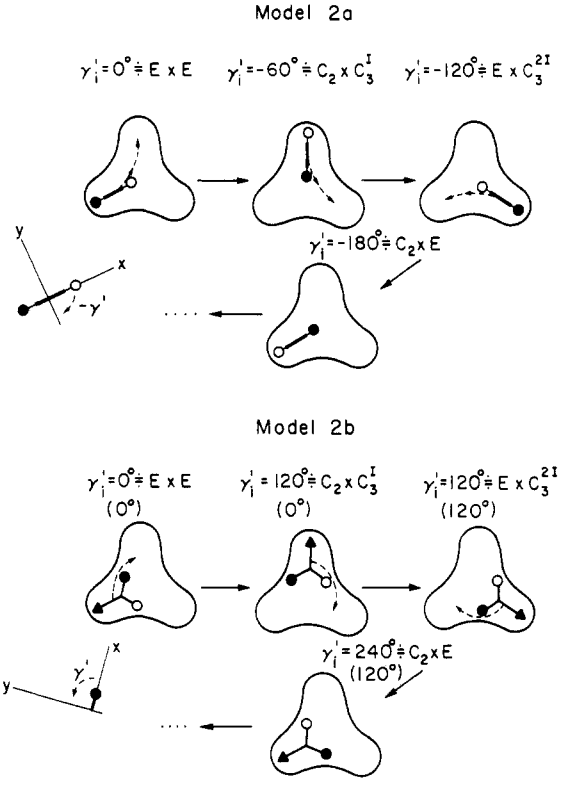

Figure 2. The three-lobed area represents a cross section through the channel, i.e. *d*, the channel axis is normal to the plane of figure. Model 2a: A molecule, with its C_2 axis parallel to the channel symmetry axis, is shown with a dark line, and the attached groups, related by C_2 molecular symmetry, are shown by open and closed circles. The dotted lines denote the trajectory of center of mass of the guest molecule during jump. Labeled on top of each figure is a product symmetry operation expressed in terms of molecular and host symmetry group elements. Model 2b: Same as 2a but the C_2 is oriented normal to C_3 axis. (See text for more details.)

In Figure 2a we illustrate one such model. We show a cross section of the host channel with three fold (C_3^H) symmetry and the "end-on" view of an *o*-xylene molecule embedded in it, such that the two ortho methyl groups are pointing toward opposite sides. The equivalence of the two ortho groups implies a C_2 molecular symmetry, and the C_2^M symmetry axis is parallel to the C_3^H host axis. [More precisely, the symmetry of the host channel is assumed to be D_{3h} while that of *o*-xylene is C_{2v}, but the additional symmetry elements are not needed to describe the motion.] In the model illustrated in Figure 2a the *o*-xylene "slides" over into an adjacent threefold lobe in the host channel to take an equivalent position to its previous one. Although this lobe can be rotated into the original lobe by the 120° (C_3^H) rotation of the host, the actual physical process only involves a rotation of the benzene by 60°, the equivalence of the new position to the former being due also to the twofold symmetry of *o*-xylene! Thus, this "jump" between two sites may be represented by group element: $C_2^M \times C_3^I$. (I stands for the inverse rotation operation.) In a similar manner all successive jumps represent effective rotations by 60°, and a total of 6 successive jumps, not 3, in the same sense, are required to return the *o*-xylene to its original position. This is a case where the direct product group is equivalent to a simple C_6 group.

In another example, shown in Figure 2b the host channel with threefold symmetry is again used, but we have an acetone molecule with its main plane symmetrically disposed in one of the channel lobes. Here the motion between adjacent lobes is an end-over flip of the C=O bond coupled with a slide into the adjacent lobe. This motion between adjacent lobes of the host channel is seen to rotate one methyl group by 120° and the other by 0°! In successive jumps between adjacent lobes, the methyl groups alternate between being rotated by 120° and by 0°, so six jumps in the same sense are required to return the acetone molecule to its original position.

(12) Spiess, H. W.; Sillescu, H. *J. Magn. Reson.* **1981**, *42*, 381.
(13) Woessner, D. E. *J. Chem. Phys.* **1962**, *1*, 36.
(14) Rananavare, S. Ph.D. Thesis, University of Missouri, St. Louis, 1983, p 263.
(15) Alexander, S. *Can. J. Phys.* **1972**, *50*, 1568.
(16) Longuet-Higgins, H. C. *Mol. Phys.* **1963**, *7*, 445.

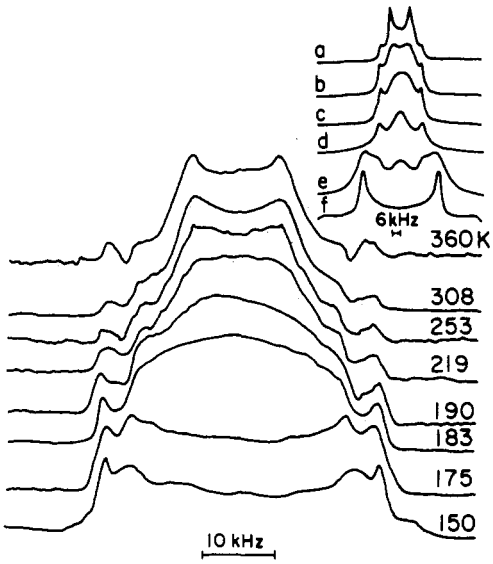

Figure 3. Experimental ^{2}H NMR spectra obtained at the temperatures denoted on figure from a polycrystalline sample of CPZ–*p*-xylene-d_{10}. The insert shows quadrupole echo line shapes calculated for discrete jumps about a C_3 symmetry axis with the time between the two 90° pulses in the quadrupole echo sequence τ_e = 30 μs, a tilt angle of 67.5° between the principal axis of an axial quadrupole tensor and the jump axis, and the following jump rates: (a) τ_j^{-1} = 0, (b) 1.2 × 10^4, (c) 3.0 × 10^4, (d) 1.0 × 10^5, (e) 1.7 × 10^5, (f) 6.7 × 10^5 s^{-1} (reproduced with permission from ref 5e).

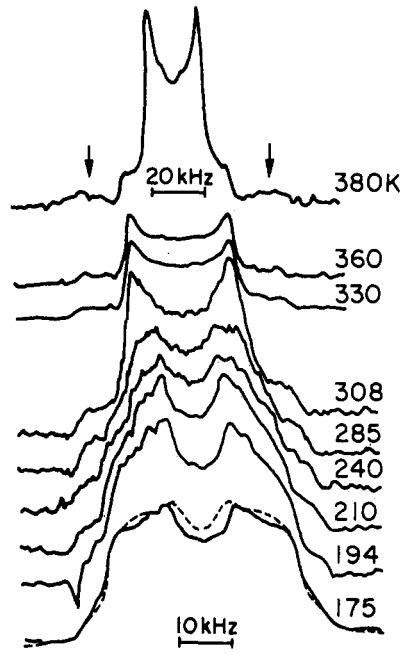

Figure 4. Figure 4 is the same as Figure 2 but for CPZ–*o*-xylene-d_{10}. The dashed line superimposed on the 175 K experimental spectrum is a powder spectrum calculated with η = 0.932 and a natural line width of roughly 5% of Q_0 (reproduced with permission from ref 5e).

There is also another, and simpler motion, within a single lobe viz. rotation of the acetone molecule about its C_2 axis (parallel to the C=O bond), which is seen to be equivalent to a rotation of one methyl by 240°, and the other by 120°. One finds that in this example the relevant direct-product group is equivalent to a simple D_3 group. It differs from the first case because the C_2^M and C_3^H axes are perpendicular. [The equivalent of this second process (i.e. a molecular twofold rotation) is not possible in terms of the first model due to the assumed steric hindrance of the host lobe to methyl groups.] Given the two types of motion possible, this second case is a more complex case kinetically. However, we are only interested in averages over equivalent (or nearly equivalent sites). Thus, the important result for this model is that each methyl group need only be averaged over three orientations: 0°, 120°, and 240°.

To summarize, the above cases correspond respectively to a parallel and perpendicular orientation of the molecular C_2 axis with respect to the C_3 host symmetry. The combined symmetries generate (sub)-groups of order six, which are equivalent to the (ismorphous) point groups C_6 and D_3, respectively.

III. Results and Discussion

A. o-Xylene–CPZ and p-Xylene–CPZ Adducts. We show in Figures 3 and 4 ^{2}H NMR spectra from polycrystalline powders of CPZ–*p*-xylene-d_{10} and CPZ–*o*-xylene-d_{10}, respectively, from (ref 5d). The dashed lines and the traces shown in the insert are calculated spectra, to be discussed below.

We shall first review the previous interpretation of these spectra, given in ref 5d. The outer low-intensity peaks in both figures (hardly visible in Figure 4) were associated with the aromatic deuterons, and the central portion of the experimental spectra, with the methyl deuterons. At the temperatures used in this study the rigid-limit 124-kHz splitting of the methyl deuterons is reduced to 40 kHz due to rapid reorientation about their C_3 axis, thereby projecting the motionally averaged, $\langle Q_{zz} \rangle$, along an axis colinear with the C–C bond, connecting the methyl group to the aromatic ring. We shall only be concerned with the further motional narrowing of $\langle Q_{zz} \rangle^{\text{methyl}}$ due to hopping of the guest molecules in the interstitial sites; hence it is convenient to define a tilt angle between $\langle Q_{zz} \rangle$ and d, the channel axis (C_3 symmetry). Both molecules were assumed to be in an upright position within the inclusion channel, with the molecular C_2 symmetry axis parallel to the channel axis d. [The temperature-induced spectral changes were interpreted by line shape simulation techniques in terms of motion about the channel axis.] The simulations were carried out using a three-site jump model ($P_1 = P_2 = P_3$) for the long molecular axis tilted at 67° with respect to the channel axis d. The temperature dependence of the experimental spectra can be explained in terms of a continuous change in the jump rate as shown in Figure 3.

For this case of *p*-xylene, the more general model that is appropriate for the combined molecular and channel symmetries is the "six-site" model of Figure 2a. Nevertheless, when the occupational probabilities are equal, rapid reorientation about a C_3 or C_6 axis leads to identical motionally averaged axial line shapes. Also, we have found indistinguishable line shapes for the two models in the slow motional regime, but one must employ a smaller jump rate for the six site as compared to the three-site model.

With *o*-xylene (Figure 4), a change in the symmetry of the reorientation process about the channel axis from threefold above 308 K to twofold below that temperature was postulated.[5d] [In this case over the whole temperature range studied, only fast motional partially averaged spectra were obtained.] Besides, considerable wobbling of the molecular C_2 symmetry axis about d and a distortion of the benzene ring from a perfect hexagon had to be assumed. The spectral consequences of the latter model are manifested as an asymmetric powder pattern, such as depicted by the dashed line in Figure 4. The arguments supporting this model are, however much less cogent than with *p*-xylene-d_{10}.

In our new interpretation, we use the six-site model of Figure 2a, and we assume that *o*-xylene is jumping throughout the temperature range investigated between the same three energy minima, compatible with the site symmetry of the CPZ lattice and twofold molecular symmetry. However, one of the three minima becomes lowered by 1–2 kcal with respect to the other two at 308°, which appears to be a phase transition temperature. The temperature-dependent relative populations of the sites are quantified by defining a population ratio R:

$$R = P_1/P_2 = \exp(E_d/kT) \exp(\Delta S/R) \qquad (6)$$

where E_d denotes the enthalpy difference between the two minima associated with sites 1 and 2. Due to the molecular symmetry, this is the only ratio that needs to be specified.

We take the *o*-xylene-d_{10} molecule to be in an upright position within the inclusion channels such that its molecular C_2 symmetry

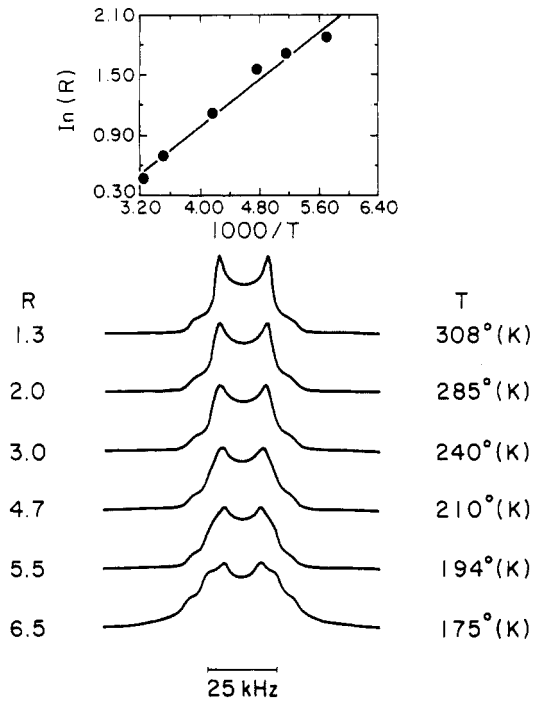

Figure 5. Simulated ^2H NMR spectra for *o*-xylene in CPZ using model 2a; tilt angle = 30°, the populations in three host sites are such that $P_1 \neq P_2 = P_3$, and R (defined in text) as function of temperature is also shown. Inset shows a log R vs. $10^3/T$ plot.

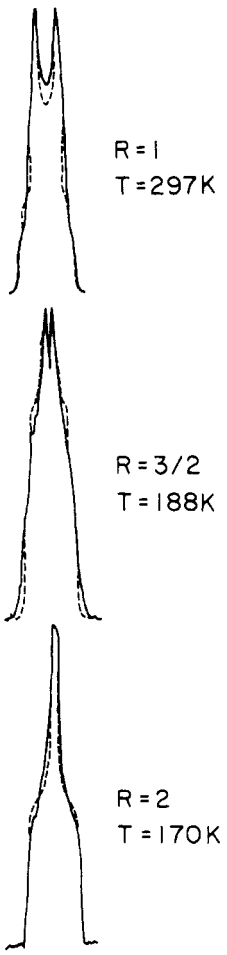

Figure 6. Experimental ^2H NMR spectra obtained from a polycrystalline powder of *o*-xylene-d_{10}–DOCA at temperatures as denoted in the figure (—). Spectra calculated for discrete jumps between two sites with relative populations R denoted in the figure, a natural line width T_2^{*-1} about 1.5% of the quadrupole constant and the mean time between jumps 10^8 s (– – –). (Reproduced with permission from ref 5h.)

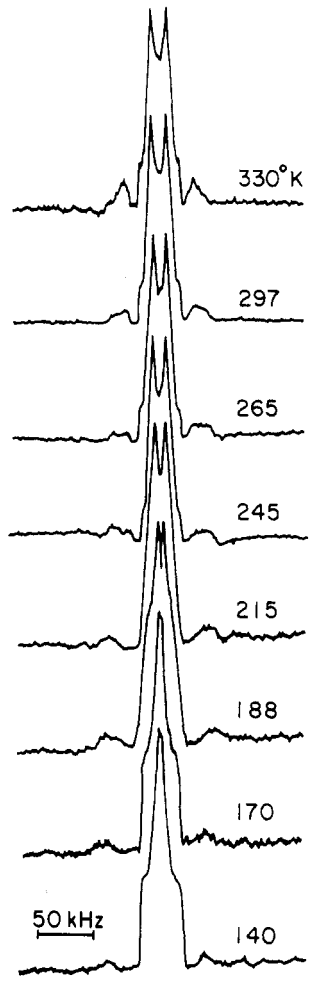

Figure 7. Experimental ^2H NMR spectra for *o*-xylene-d_{10} trapped in DOCA. The central peak doublet (narrow) is due to methyl groups while weaker outer doublet(s) are associated with aromatic deuterons.

axis is aligned along the channel axis d. This means that the aromatic to methyl C–C bond is tilted 30° with respect to the C_2 axis. Simulated spectra are shown in Figure 5, along with the population ratios. A linear log R vs. $10^3/T$ plot yields $E_d = 1.2$ kcal and $\Delta S = -2.7$ kcal/(mol K).

The sparsity of the experimental data and the simplicity of the dynamic models used do not remove all the ambiguities. For example, one may choose $P_1 \neq P_2 \neq P_3$ for all the host sites thereby defining two population ratios. The main point we wish to emphasize, however, is the simplicity and generality of our present approach. This will become increasingly clear as we proceed, showing that other cases fit into this picture.

B. o-Xylene–DOCA. We show in Figures 6 and 7 experimental ^2H NMR spectra from a polycrystalline powder of *o*-xylene–DOCA at various temperatures (solid lines), reproduced from ref 5h. These quite dramatic temperature-induced changes in the line shape were previously interpreted in terms of rapid 180° jumps about an axis tilted at 66° (or 45°), with respect to the C–CD_3 bonds, with the relative population of the two sites varying from 1 at 257 K to 2 at 170 K.

In our present analysis, we used the six-site model (Figure 2a), but we were unable to simulate the experimental line shapes (at 145–175 K) with a tilt angle of 30° between $\langle Q_{zz}\rangle^{methyl}$ and C_3 axis (guest voids) by simply increasing R (≡low temperature, cf. eq 6) values beyond the values employed in Figure 4. In the next stage of analysis, we varied the tilt angles between its limiting values, i.e. 30° ($d \| C_2^M$) and 90° ($d \perp C_2^M$); the spectra so generated as a function of R yield η values consistent with experimental spectra within a narrow range of R values. However in most cases the *overall* spectral width, especially at large R, was incompatible with low-temperature experimental spectra which clearly converge to $\eta = 1$ cf. Figure 7. At low temperatures, most of the guest

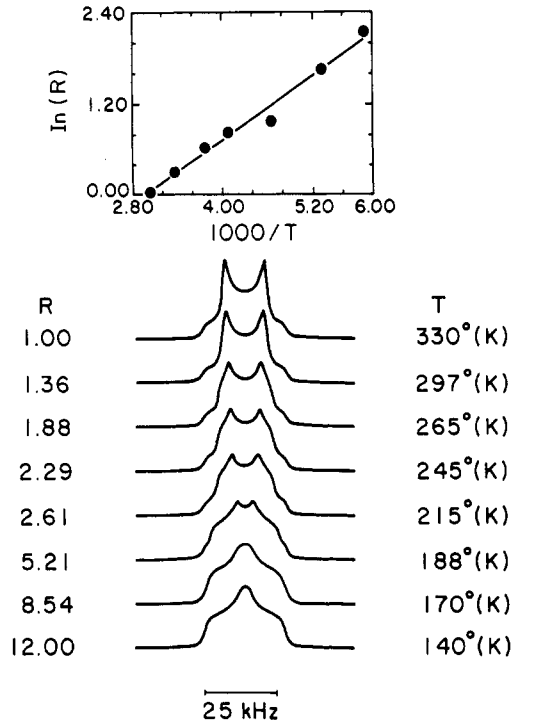

Figure 8. Simulated ^{2}H NMR spectra for *o*-xylene in DOCA using model 2a. Tilt angle = 36°. The populations in the host related sites are such that $P_1 \neq P_2 = P_3$ and R (defined in text) as a function of temperature is also shown. Inset is the same as Figure 5.

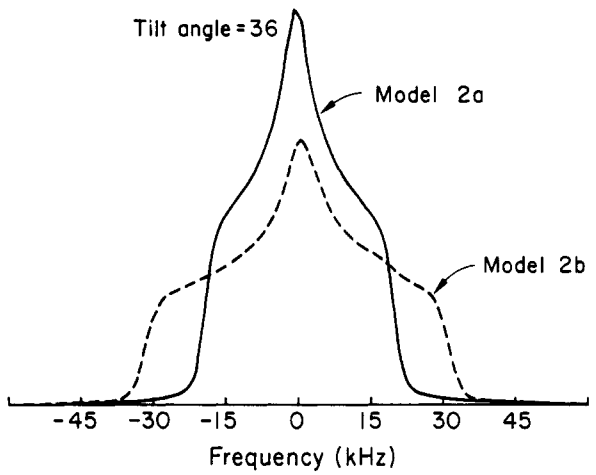

Figure 9. A comparison of model 2a vs. model 2b. Tilt angle = 36°, R = 20. Note model 2b predicts a spectrum about 50% wider than the experimentally observed spectrum at 140 K (cf. Figure 7).

molecules reside in the preferred (host related) "two" out of "six" sites, so simulated spectra should converge (for $R > 10$) to $\eta = 1$ independent of R, for a proper choice of tilt angle. After extensive search, a tilt angle of 36 ± 1° provided best-fit spectra; the results of simulations and a plot of R vs. $10^3/T$ is shown in Figure 8 (E_d = 1.4 kcal, ΔS = −4 kcal/(mol K)). In the next stage of analysis we compared the relative orientation of the C_2 and C_3 axes (see Figure 2 for models) and results for large values of R are shown in Figure 9, which clearly rule out model 2b (i.e. $C_3 \perp C_2$) since it results in larger than the experimentally observed spectral width.

Thus the overall physical picture that emerges from this new analysis is a weakly nonuniform guest–host interaction ($E_d \sim$ 1–2 kcal/mol) but with the site of lower energy corresponding to one of higher entropy (i.e. less ordered), $\Delta S \sim -3$ to −4 kcal/(mol K). Furthermore, observed fast motional ^{2}H NMR spectra down to 140 K imply a weak potential barrier for jumps (i.e. the free energy of activation, $\Delta G^{\ddagger} < 3$ kcal/mol).

C. DOCA–Acetone-d_6 and APA–Acetone-d_6. Experimental ^{2}H NMR spectra obtained at ambient temperature from polycrystalline powders of apocholic acid (APA)–acetone-d_6 and deoxycholic acid (DOCA)–acetone-d_6 are shown in parts a and d of Figure 10, respectively. These spectra were originally interpreted to reflect (besides rapid internal methyl rotation) fast exchange of the two methyl groups within a given acetone molecule and a difference in the orientation of the acetone guests within the inclusion channels of APA and DOCA, respectively. Namely, the C=O bond was assumed to be tilted relative to the channel axis by 65.5° in the APA tunnels and by 55° in the DOCA tunnels. Moreover, it was necessary to require that the two equivalent exchanging molecular orientations be unequally populated! The best fit between theory and experiment obtained with this model is illustrated by the dashed lines in Figure 10, a and d, with R = 2 denoting a 2:1 population ratio.

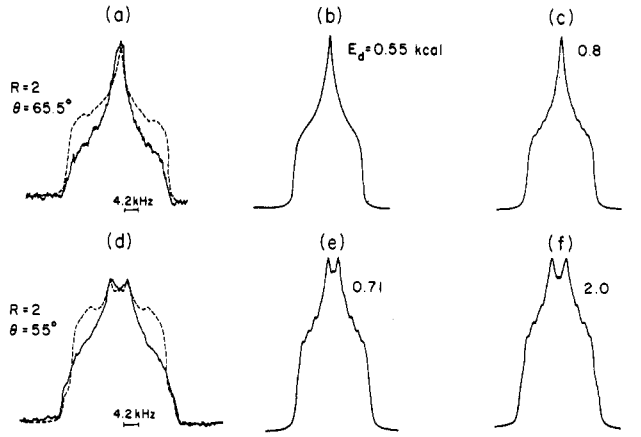

Figure 10. (a) Experimental ^{2}H NMR spectrum obtained from a polycrystalline powder of acetone-d_6–APA at ambient temperature (—); spectrum calculated for discrete jumps between two equivalent sites using the analytical expression given by Spiess and Sillescu[12] for a jump rate of 10^8 s^{-1}, a natural line width about 15% of the quadrupole constant, the tilt angle between the jump axis and the principal axis of the quadrupole tensor Q = 45° (or 66°), and the relative population of the two sites R = 2 (– – –) (reproduced with permission from ref 5f). (b) Spectrum calculated with planar threefold jumps (model 2b) between three energy minima one lowered by 0.55 kcal relative to the other two. The calculation was performed as described in the Background section. (c) Same as (b), except that two of the energy levels are lowered by 0.8 kcal relative to the third. (d) Experimental ^{2}H NMR spectrum obtained from a polycrystalline powder of acetone-d_6–DOCA at ambient temperature (—); spectrum calculated as described in the captions of Figure 6a, with θ = 55° (– – –) (reproduced with permission from ref 5h). (e) Same as the captions of Figure 6b, with E_d = 0.71 kcal. (f) Same as the captions of Figure 6c, with E_d = 2.0 kcal.

Note that the fit is not so good. Furthermore, the requirement of unequal populations of orientations equivalent by molecular symmetry cannot be correct. Also, note that a diffusion tilt β' other than 60° implies that the acetone-d_6 molecule must be tipping over within the inclusion channels so that the C=O bond and the channel axis d which, for symmetry reasons, must be parallel to the jump axis, are no longer colinear. This implies a very specific geometry, which so far has not been corroborated by other types of physical measurements.

We suggest the alternative interpretation using the models shown in Figure 2. Our initial attempt using model 2a ($C_2^M \| d$) proved unsuccessful in reproducing fast motional spectra, since the 60° tilt angle between $\langle Q_{zz} \rangle$ and d results in widths that are four times smaller than the observed widths at room temperature. Unfortunately, with only one fast motional spectrum, it is impossible to assess possible variation of tilt angles and population ratio R. From steric consideration, we chose model 2b where methyl groups are located in the center of the channel void. Differences in the spectra of APA–acetone-d_6 vs. DOCA–acetone-d_6 are then accounted for by the magnitude of the energy difference, E_d. Namely, the former spectrum can be interpreted with E_d = 0.53 kcal and the latter with E_d = 0.7 kcal.

Simulations based on this model are shown in Figure 10, b, c, e, and f. Spectra 10b and 10e were obtained with one energy level lowered by 0.55 kcal relative to the other two, whereas spectra

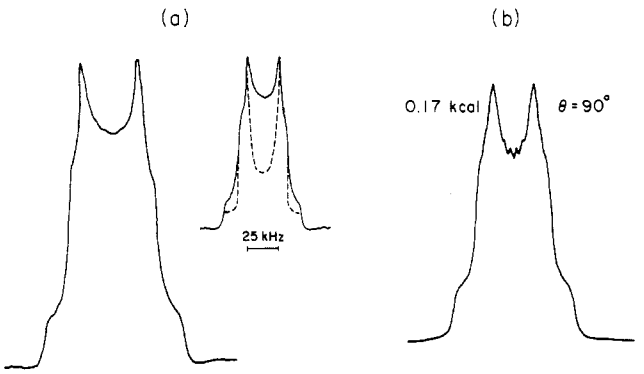

Figure 11. (a) Experimental ^2H NMR spectrum obtained from a polycrystalline powder of cyclohexanone-d_{10}-DOCA at room temperature. Insert shows the symmetric powder spectrum calculated with $Q_0 = 43.2$ kHz, $T_2^{-1} = 4$ kHz, and $\eta = 0.17$ (---); solid line as in the captions of Figure 7a (reproduced with permission from ref 5h). (b) Spectrum calculated with planar jumps as shown in Figure 2b with one host site energy level lowered by 0.17 kcal relative to the other two and a tilt angle $\theta = 90°$ between the jump axis and the principal axis of the quadrupole tensor.

10c and 10f, with two energy levels lowered by 0.8 kcal relative to the third one.

The fit between the calculated spectra in Figure 10, b, c, e, and f, and the corresponding experimental spectra in Figure 10, a and b, is superior to that achieved with the earlier twofold jump model. We expect that a series of temperature-dependent spectra above room temperature could allow one to distinguish between the two sets of energy differences we used above.

D. DOCA-Cyclohexanone-d_{10}. The ^2H NMR spectrum obtained at room temperature from a polycrystalline powder of DOCA-cyclohexanone-d_{10} is shown in Figure 11a. This was previously interpreted in terms of rapid ring inversion and fast nonuniform reorientation about the symmetry axis of the average conformer. The spectral consequences of such a model are manifested in terms of an asymmetric powder pattern, of the type shown in Figure 1c. The dashed line in the Figure 11 insert is an asymmetric powder spectrum with $\eta = 0.17$, compatible with the above-mentioned model, without, however, providing compelling evidence for its validity.

We suggest the following alternative in the spirit of our previous examples. Cyclohexanone experiences rapid ring inversion (this is most certainly correct, as we observe a single-species spectrum). The average conformer lies within the channel cross section and is hopping rapidly between three host sites (model 2b) with one of the energy minima lowered by 0.7 kcal relative to the others. We show in Figure 11b a spectrum calculated with this model, and it is seen to conform closely to experiment. Furthermore, this model is simpler and more plausible than the previous interpretation.[5]

To summarize, the interpretation we offer in this report is based on a general property, viz. the site symmetry of the host lattice. The crystal fields determine the nature of the motion of the guest molecules, but molecular symmetries will also be a contributing factor.

IV. Conclusion

We offered in this work a comprehensive interpretation of ^2H NMR spectra from polycrystalline powders of a number of channel-type inclusion compounds. From a structural viewpoint, in all the inclusion channels referred to in this work, the guest molecule occupies a three-lobed region and is engaged in jump motions. We show that the symmetry of these motions can in all cases be viewed to be controlled by a combination of the site symmetry of the host lattice, and that of the molecule.

We have also commented on the uniqueness of the interpretations reached from the approach used in this work.

Acknowledgment. This work was supported by NSF Grants CHE-8319826, DMR 86-04200, and NIH Grant GM-25862.

Electronic Spectra and Structure of a Carbocyanine-Oxonol Mixed Dye Crystal

P. D. Ries,† C. J. Eckhardt,*

Department of Chemistry, University of Nebraska—Lincoln, Lincoln, Nebraska 68588-0304

and J. R. Collins

SRI International, Menlo Park, California 94025 *(Received: November 3, 1986; In Final Form: March 31, 1987)*

The first single-crystal spectroscopic study of the ionic "gold" polymorph of 3,3'-dimethylthiacarbocyanine (DMTC) with 3,3',5,5'-tetramethyltrimethine (TMO) is reported. Specular reflection spectra at 300 K and their Kramers-Kronig transforms were obtained, and the energies and polarizations of the transitions in the 1.5-3.8-eV region have been assigned. These results compare favorably with INDO calculations of the chromophores' spectra. Deviations of the crystal spectra from those of the free molecule can be rationalized by exciton-photon (polariton) coupling.

Introduction

Previous studies of single-crystal thiacarbocyanine dyes and complexes of these dyes have demonstrated the importance of the crystal structure to optical and electronic properties.[1-3] However, the relationship between crystal structure and the strong exciton-polariton coupling found in organic dye crystals has remained largely unexplored. Etter et al. introduced a new series of mixed dye crystals which permit a systematic study of structural effects on exciton-polariton coupling.[4,5] In this system, 3,3'-di-

† Work completed in partial fulfillment of requirements for the Ph.D. at the University of Nebraska—Lincoln.

* Author to whom correspondence should be addressed.

(1) Delaney, J.; Morrow, M.; Eckhardt, C. J. *Chem. Phys. Lett.* **1985**, *122*, 425.

(2) Tanaka, J.; Tanaka, M.; Hayakawa, M. *Bull. Chem. Soc. Jpn.* **1980**, *53*, 3109.

(3) Klanderman, B. H.; Hoesterey, D. C. *J. Chem. Phys.* **1969**, *51*, 377.

0022-3654/87/2091-5020$01.50/0